Proceedings of the ASME 2017 36th International Conference on Ocean, Offshore and Arctic Engineering
OMAE2017
June 25-30, 2017, Trondheim, Norway

OMAE2017-62056

EFFECTIVE POWER AND SPEED LOSS OF UNDERWATER VEHICLES IN CLOSE PROXIMITY TO REGULAR WAVES

Stefan Daum[*]
Martin Greve
Department of Theoretical Engineering
thyssenkrupp Marine Systems
Werftstr. 112-114, 24143 Kiel
Germany
Email: stefan.daum@thyssenkrupp.com

Renato Skejic
Division of Ship Technology
SINTEF Ocean[†]
Otto Nielsens veg 10, Trondheim 7052
Norway
Email: renato.skejic@marintek.sintef.no

ABSTRACT

The present study is focused on performance issues of underwater vehicles near the free surface and gives insight into the analysis of a speed loss in regular deep water waves. Predictions of the speed loss are based on the evaluation of the total resistance and effective power in calm water and preselected regular wave fields w.r.t. the non-dimensional wave to body length ratio. It has been assumed that the water is sufficiently deep and that the vehicle is operating in a range of small to moderate Froude numbers by moving forward on a straight-line course with a defined encounter angle of incident regular waves.

A modified version of the Doctors & Days [1] method as presented in Skejic and Jullumstrø [2] is used for the determination of the total resistance and consequently the effective power. In particular, the wave-making resistance is estimated by using different approaches covering simplified methods, i.e. Michell's thin ship theory with the inclusion of viscosity effects Tuck [3] and Lazauskas [4] as well as boundary element methods, i.e. 3D Rankine source calculations according to Hess and Smith [5]. These methods are based on the linear potential fluid flow and are compared to fully viscous finite volume methods for selected geometries.

The wave resistance models are verified and validated by published data of a prolate spheroid and one appropriate axisymmetric submarine model. Added resistance in regular deep water waves is obtained through evaluation of the surge mean second-order wave load. For this purpose, two different theoretical models based on potential flow theory are used: Loukakis and Sclavounos [6] and Salvesen et. al. [7]. The considered theories cover the whole range of important wavelengths for an underwater vehicle advancing in close proximity to the free surface. Comparisons between the outlined wave load theories and available theoretical and experimental data were carried out for a submerged submarine and a horizontal cylinder.

Finally, the effective power and speed loss are discussed from a submarine operational point of view where the mentioned parameters directly influence mission requirements in a seaway.

All presented results are carried out from the perspective of accuracy and efficiency within common engineering practice. By concluding current investigations in regular waves an outlook will be drawn to the application of advancing underwater vehicles in more realistic sea conditions.

Keywords: Underwater vehicles, Submarines, Wave-making resistance, Added resistance in waves, Speed loss, Effective power, Michell thin-ship theory, 3D Rankine panel method

[*]Address all correspondance to this author.
[†]Formerly MARINTEK. SINTEF Ocean from January 1st 2017 through an internal merger in the SINTEF Group.

NOMENCLATURE

L Maximum length of submersible
D Maximum diameter (beam) of submersible
H Maximum height of submersible
S Hull surface area of submersible
V Form displacement of submersible
$\mathbf{U}$ Mean forward speed of submersible
L_W Wave length
H_W Wave height
A_W Wave amplitude
ζ Wave elevation
c Bottom clearance
s Free surface clearance
d Submergence depth
g Ground distance
α Angle of attack
ω Angular wave frequency
λ Error
Fn FROUDE number
Rn REYNOLDS number
BEM Boundary Element Method
FVM Finite Volume Method
VoF Volume of Fluid
EFD Experimental Fluid Dynamics
EFD Computational Fluid Dynamics
UV Underwater Vehicle
UUV Unmanned Underwater Vehicle

INTRODUCTION

Nowadays, the maneuvering of Underwater Vehicles (UV's) in confined waters is of increasing interest for their design to accomplish operational tasks. Novel concepts of Unmanned Underwater Vehicles (UUV's) allow complex missions without any operator input. The fulfillment of operational requirements by ensuring safety aspects at the same time is a challenging task for such types of submersibles. Similar aspects apply to conventional submarine designs, which have to meet increasing off-design conditions for motions in proximity to waves or ice as well as for near-shore maneuvers in (very) shallow water.

The hydrodynamics of axisymmetric bodies have been studied for decades in hydrodynamic research. Published results provide a fundamental basis to set one's sights on more complex geometries. Extreme cases, such as small submergence or low clearance to the sea bottom will be consequently addressed. Unfortunately, there is a lack of data, when it comes to more realistic type of geometries and that is for several reasons. To close this lack there is clearly a need of profound validation by EFD and CFD.

The main objective of this paper is to demonstrate the utilization of numerical methods to determine the added resistance of UV's in regular deep water waves by determining the effective power and speed loss, respectively. The combined boundary/initial value problem is solved for slender geometries of varying length to diameter ratios with and without fore-and-aft symmetry. Therefore, classical BEM approaches such as first order panel methods are extended to account for varying distances to the free surface. A brief comparison to FVM results for the purpose of validation will complete this study by discussing numerical aspects.

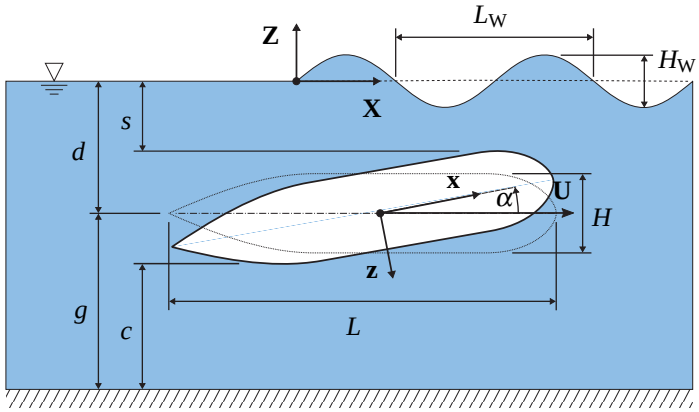

Characteristic parameters:

$\frac{d}{H} = \frac{d}{D}$ Non-dim. submergence $\frac{L}{D}$ Fineness ratio

FIGURE 1: COORDINATE SYSTEM AND MAIN PARTICULARS.

HYDRODYNAMIC PROBLEM

Coordinate System

This paper studies submersibles moving in proximity to the free surface. The underlying coordinate system is presented in figure 1. With respect to an arbitrary body fixed point C the vertical distance d to the mean free surface is called submergence depth. The origin C is chosen midship in the centerline (principal plane of symmetry) of a right-handed, Cartesian coordinate system (x,y,z) fixed with the body. The longitudinal axis x is pointing forward, y-axis is directed to starboard and z-axis vertically downwards. Main dimensions of the body are defined by the overall length L, the beam that equals the maximum hull diameter D, and the total height H that is covering all superstructure or appendages, if present.

Wave-making resistance, effective Power and speed loss

Estimation of the calm water resistance of a submerged underwater vehicle in a close proximity to the free surface is formulated on a simplified Doctors and Day [1] approach where the

total resistance R_T is expressed as:

$$R_T = R_F + R_W \tag{1}$$

with the frictional resistance R_F and the wave making part R_W. Expression (1) is based on FROUDE's hypothesis where the frictional resistance term is functionally dependent on the Reynolds number $Rn = UL/\nu$, while the wave making resistance is dependent on the Froude number $Fn = U/\sqrt{Lg}$. Here, U is the vehicle mean forward speed, L is the waterline length, g is the acceleration due to gravity ($g = 9.81\,\mathrm{m/s^2}$) and ν is the kinematic viscosity coefficient ($\nu = 1.35 \cdot 10^{-6}\,\mathrm{m^2/s}$ of seawater at 10 °C). The frictional (viscous) resistance R_F in (1) is calculated as:

$$R_F = C_F \frac{1}{2} \rho S U^2 \tag{2}$$

with the frictional coefficient $C_F = 0.075/(\lg Rn - 2)^2$ according to the ITTC'57 correlation line and water density $\rho = 1026.9\,\mathrm{kg/m^3}$ for sea water at 10 °C and the total wetted surface area S.

The estimation of wave resistance R_W is predicted by means of MICHELL's thin-ship theory, a modified version with inclusion of viscous effects according to Tuck [3] and Lazauskas [4] as well as a 3D BEM (RANKINE panel method, e.g. [8]), 3D unsteady first order BEM *pan*MARE and a fully viscous FVM.
In the following section brief descriptions of the above stated approaches are outlined dealing with the hydrodynamic problem of moving underwater vehicles close to the free-surface.

The power needed to tow an UV without its own propulsion, which experiences the total resistance R_T given by (1) at the desired mean forward speed U is called the effective power

$$P_E = |R_T| U\,. \tag{3}$$

In this paper a speed loss ΔU presents the difference between initial mean forward speed and that obtained at constant effective power P_E for given non-dimensional wavelength ratios λ/L in regular deep water waves.

Potential flow

For the present investigations of the fluid flow around moving bodies in close proximity to boundaries an ideal single phase fluid, neglecting viscosity and compressibility, is assumed. Describing the three-dimensional flow by a vector field $\mathbf{v}$ on a bounded domain $\Sigma \in \mathbf{R}^3$ that is twice continuously differentiable, Helmholtz's theorem states

$$\mathbf{v} = \nabla\phi + \nabla \times \mathbf{A} \tag{4}$$

If the flow is considered as irrotational

$$\nabla \times \mathbf{A} = \mathbf{0}\,, \tag{5}$$

then the zero-divergence vector $\mathbf{A}$ vanishes and the velocity field can be solely found by the gradient of a scalar function ϕ known as the velocity potential. The proof of this theorem can be found in [9]. Putting this statement into the continuity equation gives

$$\frac{\partial u_i}{\partial x_i} = 0 = \frac{\partial}{\partial x_i}\frac{\partial \phi}{\partial x_i} = \frac{\partial^2 \phi}{\partial x_i \partial x_i} = \nabla \cdot \nabla \phi\,. \tag{6}$$

Equation (6) is a second-order elliptic partial differential equation known as Laplace's equation for a twice continuously differentiable scalar function ϕ with

$$\nabla \cdot \nabla \phi = \mathrm{div} \cdot \mathrm{grad} \phi = 0 \tag{7}$$

The solutions of Laplace's equation are the harmonic functions derived by potential theory and valid for the whole domain bounded by Σ. Applying the divergence and GREEN's theorem to a given potential flow problem, the solution describing field can be reduced to a boundary value problem that has been numerically treated with a classical BEM further on.

APPLIED APPROACHES

Modified Michell wave theory

A submerged UV is assumed to be advancing on a steady straight line course at constant speed and diving depth. Based on potential flow theory and in the reference frame travelling with the vehicle, it can be shown (see for instance [2]) that the wave-making resistance R_W can be expressed as:

$$R_W = -\frac{4}{\pi}\rho U^2 \nu^2 \int_1^\infty \frac{\lambda^2}{\sqrt{\lambda^2 - 1}} |A(\lambda)|^2 \,\mathrm{d}\lambda \tag{8}$$

with

$$A(\lambda) = -i\nu\lambda \iint_{cp} \zeta(x,z) \exp\{\nu z \lambda^2 + i\nu x \lambda\}\,\mathrm{d}z\mathrm{d}x - \int_{-T}^{0} \zeta\,(x_s,z) \exp\{\nu z \lambda^2 + i\nu x_s \lambda\}\,\mathrm{d}z \tag{9}$$

where $A(\lambda)$ represents the complex wave amplitude. In the following, if the wave resistance is estimated according to (8), the authors refer to the MICHELL model [10].

The expression (8) can be modified with the inclusion of viscosity effects. As shown by [2] the modification can be performed by using a model by [3] and [4]. In the former one, the wave resistance R_W is given as:

$$R_W = -\frac{4}{\pi}\rho U^2 v^2 \int_1^\infty \frac{\lambda^2}{\sqrt{\lambda^2-1}}\left[\frac{\alpha}{\pi}\int_0^\infty \frac{\lambda^2 q^5}{(q-1)^2+\alpha^2\lambda^{10}q^6}|A(\lambda q)|^2\,\mathrm{d}q\right]\mathrm{d}\lambda \tag{10}$$

with

$$A(\lambda q) = -iv\lambda q \iint_{cp} \zeta(x,z)\exp\{vz\lambda^2 q + ivx\lambda\}\,\mathrm{d}z\mathrm{d}x - \int_{-T}^{0} \zeta\,(x_s,z)\exp\{vz\lambda^2 q + ivx_s\lambda q\}\,\mathrm{d}z \tag{11}$$

where α is the non-dimensional viscosity factor according to Tuck [3], which is dependent on the mean forward speed U. Similarly, the latter model according to [4], the wave resistance is formulated as:

$$R_W = -\frac{4}{\pi}\rho U^2 v^2 \int_1^\infty \frac{\lambda^2}{\sqrt{\lambda^2-1}}\left[\frac{\beta}{\pi}\int_0^\infty \frac{\lambda^3 q^4}{(q-1)^2+\beta^2\lambda^6 q^4}|A(\lambda q)|^2\,\mathrm{d}q\right]\mathrm{d}\lambda \tag{12}$$

with $A(\lambda q)$ identical to that one of (11) where β is the non-dimensional viscosity factor according to Lazauskas [4], which is also dependent on the mean forward speed U. It should be noted that in the following section the authors refer to the Tuck viscosity model or Lazauskas viscosity model if the wave making resistance R_W is predicted according to (11) or (13), respectively. In both expressions v is defined as $v = g/U^2$, index S indicates the transom stern section (if present) and the viscosity factors are defined as $\alpha = t/Fn^5$ and $\beta = t_1/Fn^3$, respectively. Here, the non-dimensional factors, t and t_1, independent of the vehicle mean forward speed U, are expressed as $t = 2(m/r)sg^{-0.5}L^{-2.5}$ and $t_1 = 4v_t g^{-0.5}L^{-1.5}$. All values of these parameters are given in SI units. In the limits $\alpha,\beta \to 0$ it can be shown that the viscosity models expressed by (11) or (13) retrieve the ordinary Michell model (without the viscosity corrections).

The outlined expression above include a simplified formulation for the source strengths (see for instance [11] and [4]) in comparison to the Havelock sources evaluated in [12], see also [13], [5], [14] [15]. Therefore, it can be normally expected that evaluation of the wave resistance according to Michell wave theory is less quantitatively accurate then more advanced method. The l and q integrals above are numerically treated by adopting the procedure described in [16]. Accordingly, the singularity of the generalized integrand $\mu^2|A(\mu)|^2/\sqrt{\mu^2-1}$ can be separated, so that:

$$\int_1^\infty \frac{\mu^2|A(\mu)|^2}{\sqrt{\mu^2-1}}\mathrm{d}\mu = \Big[|A(l)|^2\ln\left(2+\sqrt{3}\right) + \int_1^2 \frac{\mu^2|A(\mu)|^2-|A(1)|^2}{\sqrt{\mu^2-1}}\,\mathrm{d}\mu + \sum_{n=1}^{\infty}\int_{2^n}^{2^{(n+1)}} \frac{\mu^2|A(\mu)|^2}{\sqrt{\mu^2-1}}\,\mathrm{d}\mu\Big] \tag{13}$$

where μ represents the generalized integration variable and $A(\mu)$ is the generalized complex amplitude. Furthermore, concerning the numerical integration of the surface integrals (double cp integrals over the UV wetted surface S) and single integrals for ships with transom stern with a highly oscillatory integrand, the current authors also adopted the numerical technique given in [16]. It should be noted that additional details of the numerical integration procedure are not given here.

Boundary Element Method (BEM)

Submerged UV's in a close proximity to the free surface are in this paper assumed to be advancing on a steady straight line course with constant mean forward speed U and diving depth, see figure 1. The fluid velocity is described by the velocity potential ϕ, which satisfies Laplaces equation (6) in the fluid domain, meaning that the fluid is assumed to be non-viscous, homogeneous and incompressible with non-rotational flow [17]. The boundary-value problem is solved through determination of the source distribution presented by the surface (panel) integral of the source density function times the GREEN function that is given in form of Rankine sources (singularities), see [5]. This method is referred to as a 3D Rankine panel method. With the solution of the source density in hand, the wave-making resistance R_W is found from the integration of the x-component of the hydrodynamic pressure acting on the body. While the free surface elevation $\zeta(x,y)$ follows from the linearized dynamic free surface boundary condition, see e.g. [2].

Figure 2 illustrates the application of 3D Rankine panel methods on a submerged prolate spheroid studied by [18] and [19]. The spheroid is submerged at depth $d = 1.3\cdot D$ and defined by the following parameters $a/b = 5.0$, $b = c$ and $e = \sqrt{a^2-b^2}$. Here, a presents half the length of major axis, b and

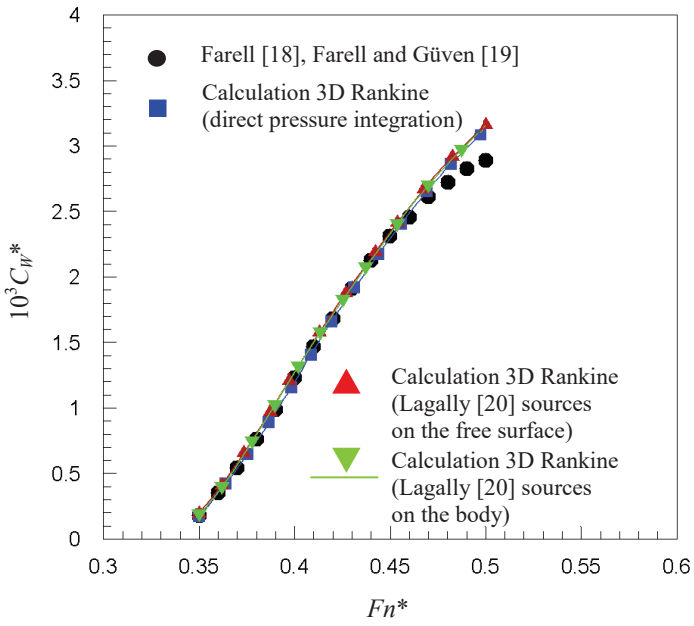

FIGURE 2: NON-DIMENSIONAL WAVE-MAKING RESISTANCE C_W VERSUS FROUDE NUMBER Fn IN CALM DEEP WATER FOR A PROLATE SPHEROID, SUBMERGED AT DEPTH $d = 1.3 \cdot D$.

c are the half length of minor axes, while e represents focal distance of spheroids.

Calculations of the wave making resistance R_W are carried out by using three different approaches. One of them is the direct pressure integration, while the other two utilize the LAGALLY [20] theorem by taking source distributions on the body and the free surface into account. This is done in order to recheck calculations carried out by the direct pressure method and, as well as, qualitative and quantitative quadrilateral panel mesh discretization of the boundary surfaces, i.e. the body and free surface are accounted by the boundary value problem described above. The calculated results are compared in figure 2 with data provided by [18] and [19]. It can be noticed that excellent agreement is achieved.

As an alternative to the previously method the authors also used a second 3D panel method which refers to the unsteady low order boundary element method, called *pan*MARE developed at Hamburg University of Technology. In addition to Rankine sources a dipole is imposed on every panel when a lift-generating body is computed, see e.g. Hundemer [21]. The boundary condition is successively solved for the Kutta condition, see [22] which states, that the fluid flow leaves the trailing edge smoothly and the fluid velocity is finite. This requires that the pressure on both sides of the trailing edge equal. Thus, a circulation leaves the lifting body at its trailing edge resulting in lift and drag forces in a potential fluid flow.

The unsteady free surface boundary conditions [23] are imposed by using a moving frame of reference together with the body. This formulation facilitates a robust implementation of effects due to long crested waves or wave spectra. In order to get a numerical solution of the flow-problem the boundaries are discretized with 3D panels and the boundary conditions are imposed in every collocation point of each panel center. The unknown source strength is determined a priori of setting up the equation system by using a Neumann type boundary condition and in every panel collocation point an equation is set up using a Dirichlet type boundary condition in order to determine the unknown doublet strengths, e.g. see [21], [24].

Finite Volume Method (FVM)

This section describes the applied Finite Volume method (FVM) with following two main properties. First, the method is based on discretizing the integral form of governing equations for two phase fluids (air/water) over each control volume. The basic quantities, such as mass and momentum, will therefore be conserved at the discrete level. Second, all equations are solved in a fixed Cartesian coordinate system on a mesh that does not change in time by treating the systems of partial differential equations in the segregated way.

In comparison to the used potential flow methods FVM discretizes the whole control volume of fluid. This allows to include shear stress and turbulence models with an arbitrary range of complexity at the vehicles wake, but on the costs of increasing computational effort.

Since for the resistance problem of submerged vehicles in general, where viscous forces are by far dominating pressure forces in deep diving conditions this balance is assumed to vary as a function of submergence when the motion in proximity to the free-surface is calculated. To include viscous forces Reynolds-averaged Navier-Stokes (RANS) equations have proven to be suitable for simulations of submerged bodies from model- to full-scale, see e.g. [25], [26].

The applied RANS equations in this paper are discretized using a polyhedral FVM, first to second order in space and time with cell-centered, colocated (or non-staggered) stored values. The equations are usually solved with a segregated pressure-based algorithm. Pressure-velocity coupling is achieved using a merged PISO-SIMPLE approach, see e.g. [27].

For the wave resistance problem the primary wave field needs to be calculated. In this paper the so-called Volume of Fluid (VoF) approach [28] is used by solving the RANS equations for 2 incompressible, (isothermal, immiscible) fluids to determine the interface based on this capturing approach. Therefore in each finite volume a scalar called phase-fraction is set to identify the water and air phase, respectively.

In both cases with Reynolds (Rn) number ranges between 10^6 to 10^8 of all used geometries, turbulence is modelled using

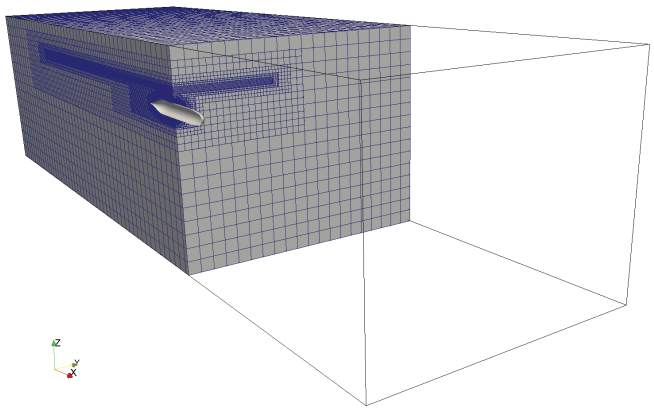

FIGURE 3: LONGITUDINAL CUT THROUGH THE COMPUTATIONAL MESH FOR THE FVM BASED VOF APPROACH OF THE SUBMERGED DARPA SUBOFF.

the k-omega-SST model. The near-wall treatment varies depending on the height of the first cell at the hull, expressed by the non-dimensional y+ value. For $y+ < 5$, the turbulence model is applied down to the wall and the boundary layer is considered fully resolved. For $y+ > 30$, a wall function is employed to model the turbulent flow adjacent to the wall. A blending function is applied for intermediate $y+$ values.
For the VoF-approach an unstructured mesh is used in all cases with sufficient local refinement of the air/water interface as well as the near-wall region of the UV. An example can be seen in figure 3 for the DARPA SUBOFF bare hull.

CASES

In this section relevant case studies are introduced. One key element for calculating the added resistance of UVs is the determination of mean second order wave loads on submerged bodies. In [29] measurements for a long slender cylinder are used to validate the current approach described in the previous section. Some details of this cylinder are outlined in the next paragraph. After that studies based on spheroids are presented. Finally, the DARPA SUBOFF as one submarine hull is described.

Cylinder

Published results of wave drift forces for slender submerged structures are still rare, but data for one horizontal cylinder are available. The principal dimensions of this cylinder according to [29] and [30] are $L = 75.6\,\mathrm{m}$ and $D = 8.4\,\mathrm{m}$ with a form displacement of $V = 4034m^3$. These particulars corresponds to medium sized conventional submarines at full-scale and should provide comparable wave drift forces. Figure 4 shows the used panel grid layout for a submergence equally to its diameter. It can be seen that the cylinder has spherical ends on both sides, so

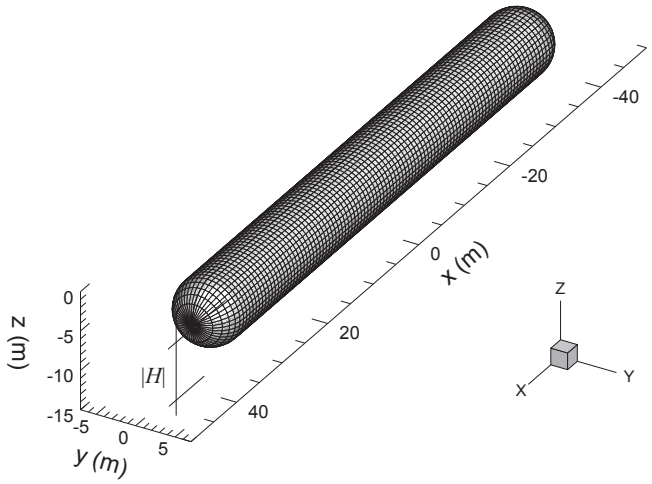

FIGURE 4: PANEL DISTRIBUTION FOR A CIRCULAR CYLINDER IN CLOSE PROXIMITY TO THE FREE SURFACE.

it is completely symmetric.

Spheroid

One of the most chosen analytical geometries, prolate spheroids provide a reasonable approximation of UV's in terms of slenderness and form displacement. As in case of the horizontal cylinder above, spheroids inherit fore-and-aft symmetry, which is not present for advancing UV's on the other hand. But, for the added resistance problem it shall be still provide results of practical importance.

In this paper spheroids having different slenderness ratios L/D between 4 to 12 with a fixed length of $L = 4\,\mathrm{m}$ are studied in different submergence depths. In table 1 main particulars of all investigated spheroid geometries are given. Both the wave-making and added resistance in regular head waves were calculated.

TABLE 1: MAIN PARTICULARS OF INVESTIGATED SPHEROIDS WITH A FIXED LENGTH OF $L = 4\,\mathrm{m}$.

		Slenderness or fineness ratio L/D					
Particular		4	5	6	8	10	12
D	[m]	1.00	0.80	$0.\overline{66}$	0.50	0.40	$0.\overline{33}$
S	[m^2]	10.12	8.03	6.66	4.97	3.97	3.30
V	[m^3]	2.09	1.34	0.93	0.52	0.34	0.23

DARPA SUBOFF

An available hull form that represents submarines is the DARPA SUBOFF. This geometry was subject to a coordinated Computational Fluid Dynamics (CFD) program to assist in the development of advanced submarines for the future. For validation purposes a variety of experimental campaigns (wind tunnel and towing tank testing) were performed as a reference for numerous numerical investigations, i.e. [25], [26] to name some recent ones.

In this paper only the axisymmetric bare hull was used, but it has not fore-and-aft symmetry as the hull forms described above. Thus, it can be recognized as a better approximation to realistic hull shapes and serves as a hull form for generic underwater vehicles. UUV's for instance are usually designed as an axisymmetric hull equipped with control surfaces.
The main advantage of the DARPA SUBOFF is that all hull lines are based on analytical expressions and can be reproduced at any time. Main particulars of the SUBOFF model are described in [31]. At model-scale the submarine has a length of $L = 4.356m$, a diameter of $D = 0.508m$ and process form displacement of $V = 0,708m^3$ with a total wetted surface area of $S = 5.998m^2$.

RESULTS

This section discusses estimation of the wave-making and total resistance of UVs according to used theoretical models. For all introduced geometries studies have been performed to analyze the calm water resistance depending on speed and submergence as well as the added resistance in regular deep water waves.

Wave-making resistance Spheroids as a simplified underwater geometry were studied for decades. A significant analytic approach of their wave resistance problem was published in [32]. Another analytical approach for spheroids was presented in [18] and compared to extensive model tests in [19]. Based on these data validation of the used panel method has been performed. Comparison for a slender spheroid with fineness ratio of 8 is shown in figure 5 at three non-dimensional submergence depths $d/D = 0.5$, 0.75, and 1.0, while results of *pan*MARE for slenderness ratios of 4.5, 6, and 8 at one draft are presented in [23]. All BEM results are close to measurements in the Froude number range tested. For low speeds no EFD data are available.

The wave-making resistance of the DARPA SUBOFF was experimentally tested at Australian Maritime College (AMC) underpinned by calculations that are published in [33], [34], and [12]. In the full range of Froude numbers relevant for UV's comparison of the Michell model and applied BEM to published results is shown in figure 6 for a non-dimensional submergence depth of $d/D = 1.1$. The non-dimensional calm water resistance is defined by $C_W = |R_W|/\rho 0.5 U^2 S$.
It can be recognized that the Michell model significantly underestimates the wave resistance, but is still able to identify the local extrema. Results based on the applied 3D Rankine panel method agree with published data in [12]. Both mildly underestimate the first local extrema at $Fn = 0.215$ and then matches experimental data starting from the first local minima at $Fn = 0.26$ until to ap-

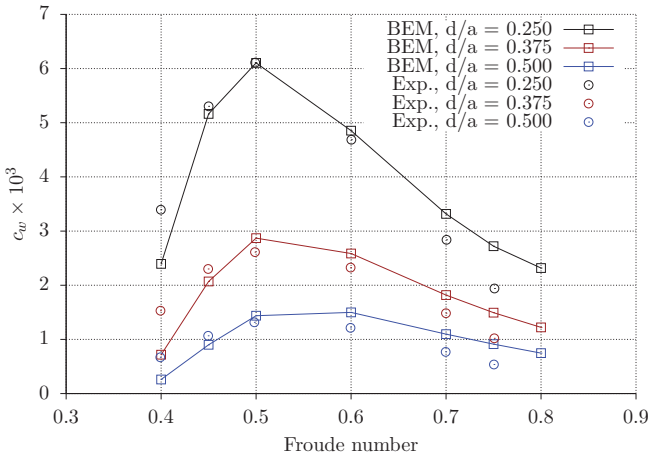

FIGURE 5: VALIDATION RESULTS OF A SPHEROIDS WAVE-MAKING RESISTANCE AT THREE NON-DIMENSIONAL SUBMERGENCE DEPTHS $d/D = 0.5$ ($d/a = 0.25$), 0.75 ($d/a = 0.375$), and 1.0 ($d/a = 0.5$).

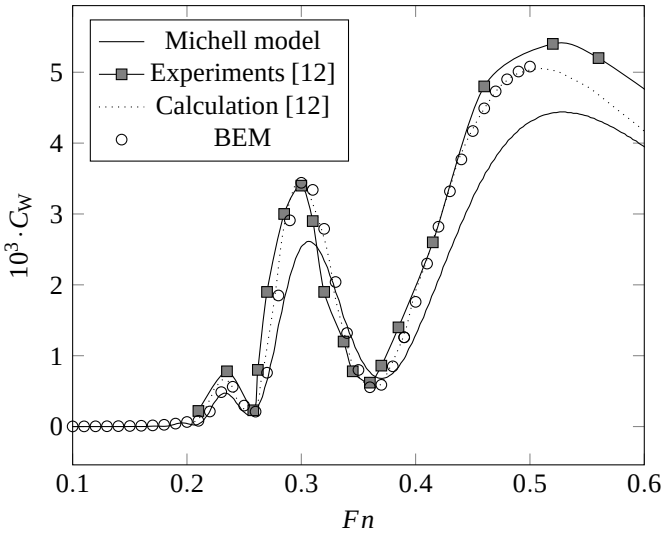

FIGURE 6: NON-DIMENSIONAL WAVE-MAKING RESISTANCE VS. FROUDE NUMBER IN CALM DEEP WATER FOR THE DARPA SUBOFF AT NON-DIMENSIONAL SUBMERGENCE DEPTH $d/D = 1.1$.

prox. $Fn = 0.4$ before starting to underestimate again at higher speeds.

For low Froude numbers around 0.2, where the wave making starts to develop, potential flow results are in general underestimating the resistance, as can be seen in figure 7 that compares the used BEM and FVM results to EFD [33] data. The wave field calculated with BEM including indicated Kelvin angle are depicted in figure 8, respectively. Since conventional submarines for instance are usually cruising at these speeds an improvement is needed. As already pointed out by Tuck [3], the effect of surface viscosity is highest at low Froude numbers. To account for viscosity effects artificial corrections in form of viscosity coefficients added to the Michell model were introduced in [3] and [4]. Figure 9 shows family of curves for different viscosity coefficients of both models in the same Froude number range as in figure 6. The figure illustrates that presence of viscosity effects has a significant influence on the resistance curve behavior. Humps and hollows in the Michell model are diminishing with gradually increased (constant) values of viscosity coefficients α and β. At low Froude numbers $Fn < 0.2$ the modified Michell models gives for more physical results in terms of C_W in magnitude, but tends to dampen local extrema in the middle Froude number range $0.2 \leq Fn < 0.5$. Thus, a correction by constant viscosity coefficients cannot be applied at higher speeds.

Added resistance The mean second order wave drift forces on the horizontal Cylinder according to [29] are calculated at zero forward speed and are directly dependent on corresponding body motions. In regular deep water head waves figure 10 presents results of the used BEM in comparison to the published data. In general the measurements could be reproduced over the relevant range from long to short waves. Best fit was achieved for pitch motions ξ_5, while heave ξ_3 is underestimated for a short range of angular wave frequencies. Unfortunately, no EFD data for surge ξ_1 referring to the added resistance in head waves are available.

For operational scenarios of UV's with near-surface motion (i.e. forward speed) seaway effects will become more important, if the submergence depth is decreasing. This applies for instance to conventional submarine, when snorkeling during transits or to smaller vehicles such as gliders when performing near-surface tasks. While natural sea environments are mostly characterized by irregular waves this paper is dealing with regular ones to study general properties.

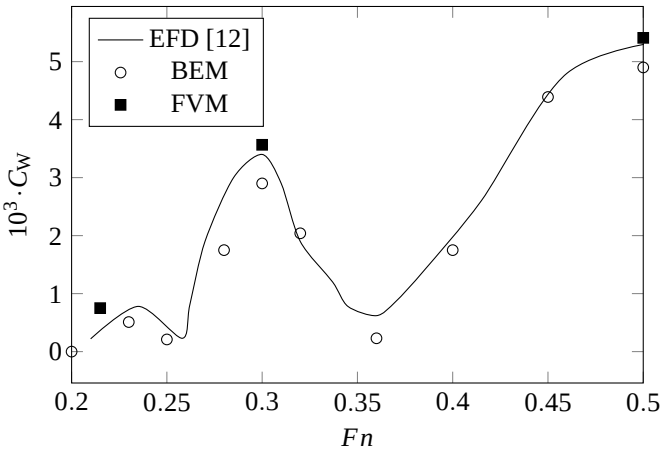

FIGURE 7: NON-DIMENSIONAL WAVE-MAKING RESISTANCE CALCULATED WITH BEM AND FVM IN COMPARISON TO EFD FOR THE DARPA SUBOFF AT NON-DIMENSIONAL SUBMERGENCE DEPTH $d/D = 1.1$ IN CALM DEEP WATER.

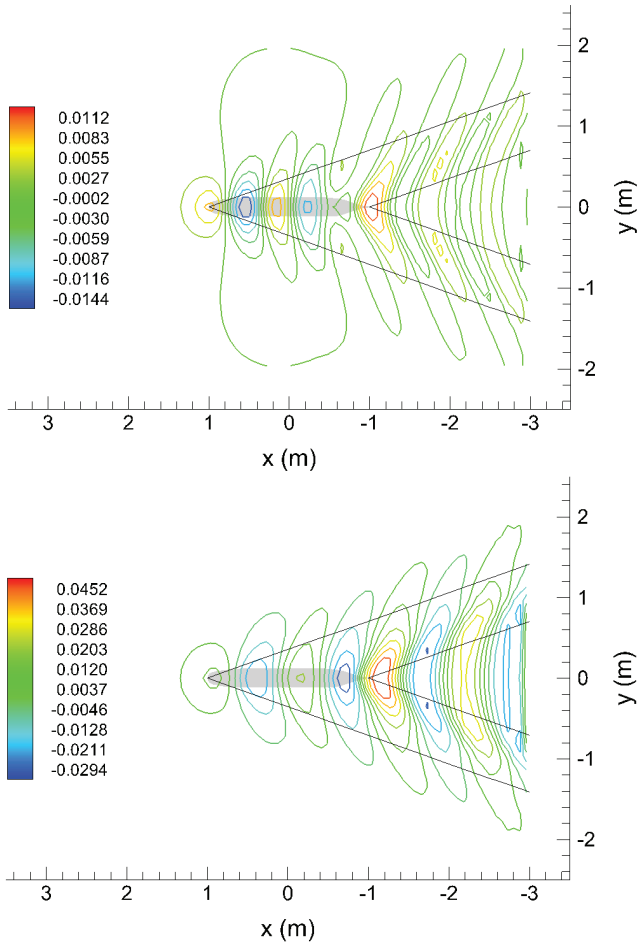

FIGURE 8: WAVE FIELD CALCULATED WITH BEM FOR THE DARPA SUBOFF AT NON-DIMENSIONAL SUBMERGENCE DEPTH $d/D = 1.1$ IN CALM DEEP WATER AT $Fn = 0.25$ AND 0.3.

At the lowest submergence depth $d/D = 1.1$ measurements of DARPA SUBOFF in [33], where wave effects will be most pronounced the added resistance is calculated at selected Froude numbers as a function of different wave lengths. In figure 11 the added resistance at $Fn = 0.25$ and $Fn = 0.3$ is compared over a non-dimensionl wave length range from $0,\ldots,2.5$. It can be observed that values for $Fn = 0.25$ are higher than in the case of $Fn = 0.3$. This is due to the fact that UV's body motions in the vertical plane, as shown in figure 12, are higher for lower Froude numbers. If we now recall that the value of the mean second order surge force (added resistance) is dependent on body motions it follows that added resistance at lower and higher Froude numbers are reversely proportional. This is completely opposite to surface vessels, when similar analysis would be performed, see e.g. [35].

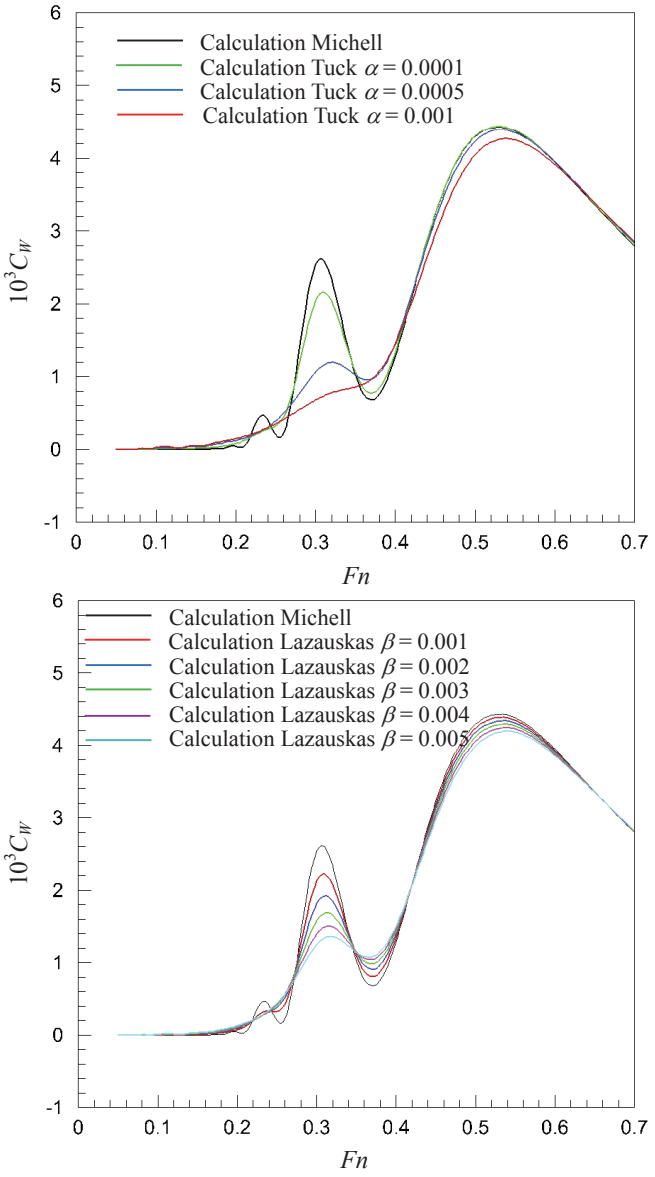

FIGURE 9: VISCOSITY EFFECTS IN COMPARISON TO THE ORDINARY MICHELL MODEL.

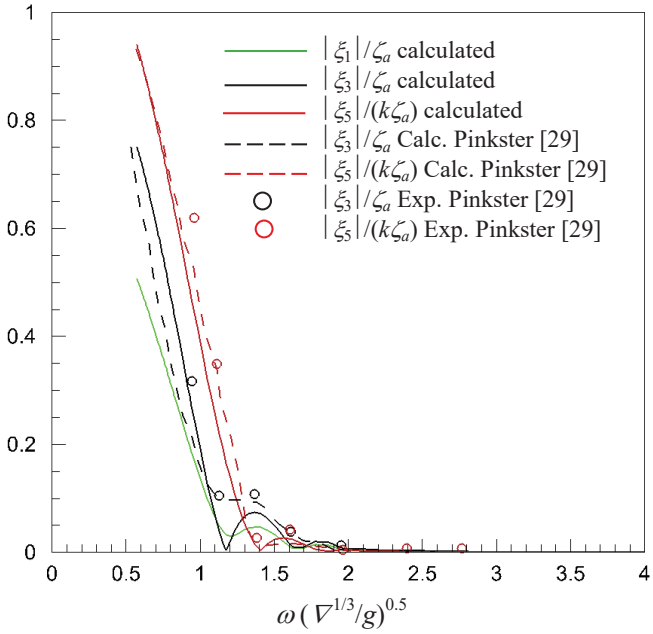

FIGURE 10: SURGE ξ_1, HEAVE ξ_3, AND PITCH ξ_5 MOTION OF A HORIZONTAL CYLINDER IN REGULAR DEEP WATER HEAD WAVES, SUBMERGED AT $d/D = 1.0$.

Effective Power and speed loss The effective power (3) was calculated for axisymmetric hulls based on the total resistance R_T as sum of the wave making part and the added resistance in regular deep water waves. Figure 13 presents results for the DARPA SUBOFF in a Froude number range of $0.1 \leq Fn \leq 0.4$ for two non-dimensional wavelength ratios $\lambda/L = 0.75$ and 1.25 at lowest non-dimensional submergence depth $d/D = 1.1$. Humps and hollows of the calm water resistance curve are still significant. All curves approaching zero at $Fn = 0.0$ as expected. At low speeds ($Fn \leq 0.14$) shorter waves will lead to higher effective power than longer waves. For speeds above that Froude number this trend is reversed and remains until high speeds. Maximum difference of the effective power is reached at local wave making extrema, while minimum difference is found at maximum slopes of the resistance curve.

The speed loss was then calculated at constant effective power P_E and at given non-dimensional wavelength ratios λ/L in an interval of the incident regular wave amplitudes of $\zeta \in [1.0;6.0]$ m. It should be noted that when $\zeta = 0$ m the submarine advances forward on the straight line course at initial

Froude number and the speed drop is zero, respectively. Figure 14 compares speed drops ΔU for the DARPA SUBOFF at lowest submergence $d/D = 1.1$ for two speeds $Fn = 0.25$ and 0.3 as in figure 11 for the two different non-dimensional wavelength ratios $\lambda/L = 0.75$ and 1.25, as in figure 13. When moving with lower speeds the speed drop is significantly pronounced with increasing wave height. In general longer incident waves will lead to higher speed losses.
In the range of incident wave amplitudes $\zeta \in [0.0; 1.0]$ m (not shown in figure 14) it has been observed that speed drop curves have quite different slopes compared to them at higher wave amplitudes. This might be nonphysical and these results are excluded here, while to be subject of further analysis.

CONCLUSION

This study addresses the theoretical prediction of the effective power and speed loss of underwater vehicles in close proximity to regular waves.

The power requirements of underwater vehicles have been derived from a modified version of the Doctors & Day method [1], which predicts the total resistance. The introduced modifications are mainly related to different methods of estimating the calm water resistance according to various wave theories in which the influence of viscosity effects was studied in some detail. In particular, the modified Michell wave theory by inclusion of viscosity correction factors was introduced for the first time with applications to underwater vehicles and their effects on the wave-making resistance. It has been analyzed that the influence of viscosity effects on the prediction of the calm water resistance become important, especially in the lower range of Froude numbers. Insight into the free-surface wave profiles for selected cases were provided by two 3D Rankine panel methods supplemented with fully viscous simulation results.

Validation and verification were performed by comparison to experimental and numerical data for axisymmetric underwater hull forms. In close proximity to the free surface seaway effects are significant for the motion of underwater vehicles. The added resistance in regular deep water waves is calculated for selected cases. Remarkably, longer waves at lower speeds lead to higher added resistance of a submerged body at constant forward motion. This fact is opposite to surface vessels or surface piercing bodies in general. Based on these results the effective power and speed loss in regular deep water waves are studied.

On the whole, the majority of obtained results show satisfactory agreement with published data in the range of suitable Froude numbers. At low speeds the accuracy of predicting the

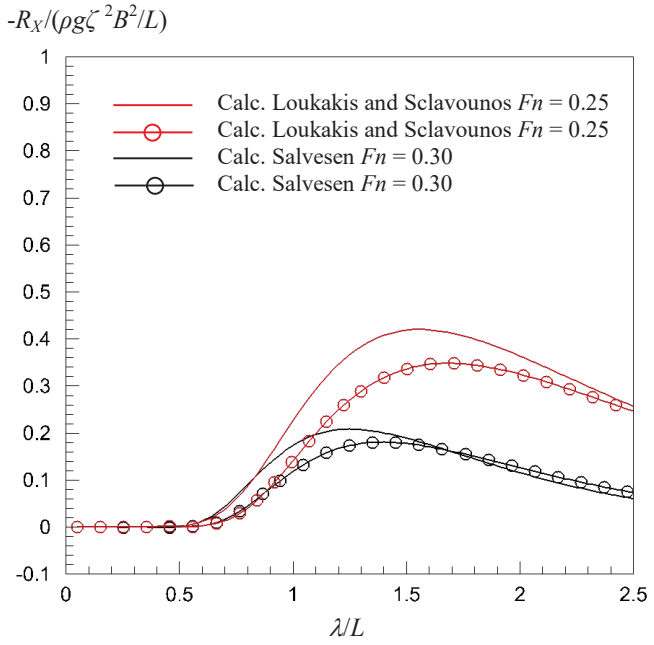

FIGURE 11: ADDED RESISTANCE (SURGE MEAN SECOND ORDER DRIFT FORCE) IN INCIDENT REGULAR HEAD DEEP WATER WAVES VERSUS NON-DIMENSIONAL WAVELENGTH RATIOS λ/L FOR THE DARPA SUBOFF AT SUBMERGENCE DEPTH $d/D = 1.1$, AT FROUDE NUMBERS. $Fn = 0.25$ AND $Fn = 0.3$.

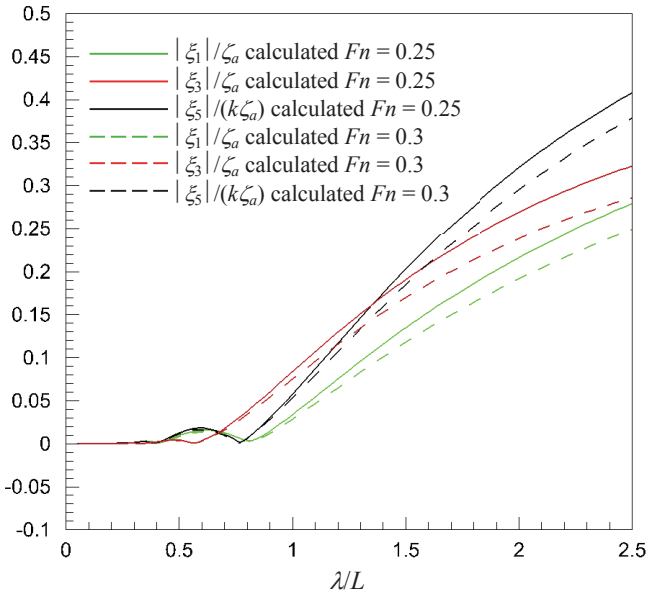

FIGURE 12: VERTICAL MOTIONS ζ_1 (SURGE), ζ_3 (HEAVE) AND ζ_5 (PITCH) IN INCIDENT REGULAR HEAD DEEP WATER WAVES VERSUS NON-DIMENSIONAL WAVELENGTH RATIOS λ/L FOR THE DARPA SUBOFF AT SUBMERGENCE DEPTH $d/D = 1.1$ AT FROUDE NUMBERS: $Fn = 0.25$ AND 0.3.

wave-making resistance is challenging for all used numerical methods. While this paper is dealing with submerged vehicles in regular waves, projections for more realistic scenarios in natural seaways are drawn.

ACKNOWLEDGMENT

Current work was performed at SINTEF Ocean and thyssenkrupp Marine Systems to which the authors express their gratitude for financial support of the R&D project on theoretical investigations of underwater vehicle performances in deep water close to waves.

REFERENCES

[1] Doctors, L., and Day, A., 1997. "Resistance Prediction for Transom-Stern Vessels". In Proceedings of FAST97, N. Baird, ed., Vol. 2, pp. 743–750.

[2] Skejic, R., and Jullumstrø, E., 2012. "Power Performance and Environmental Footprint of High-Speed Vessels in Calm Deep Water". *ASME 2012 31st International Conference on Ocean, Offshore and Arctic Engineering*, ***4***(OMAE2012-83343), July, pp. 381–393.

[3] Tuck, E. O., 1974. "The Effect of a Surface Layer of Viscous Fluid on the Wave Resistance of a Thin Ship". *Journal of Ship Research*, ***18***(4), Dec., pp. 265–271.

[4] Lazauskas, L. V., 2009. "Resistance, Wave-Making and Wave-Decay of Thin Ships, with Emphasis on the Effects of Viscosity". PhD thesis, University of Adelaide, School of Mathematical Sciences.

[5] Hess, J. L., and Smith, A. M. O., 1962. Calculation of Non-Lifting Potential Flow about Arbitrary Three-Dimensional Bodies. Report 40622, Douglas Aircraft Company.

[6] Loukakis, T. A., and Sclavounos, P. D., 1978. "Some Extensions of the Classical Approach to Strip Theory of Ship Motions, Including the Calculation of Mean Added Forces and Moments". *Journal of Ship Research*, ***22***(1), Mar., pp. 1–19.

[7] Salvesen, N., Tuck, E. O., and Faltinsen, O. M., 1970. "Ship Motions and Sea Loads". Vol. 78, pp. 250–287.

[8] Skejic, R., 2008. "Maneuvering and Seakeeping of a Single Ship and of Two Ships in Interaction". PhD thesis, Faculty of Engineering Science and Technology, Norwegian University of Science and Technology.

[9] Newman, J. N., 1977. *Marine Hydrodynamics*. MIT Press, Cambridge.

[10] Michell, J. H., 1898. "The Wave-Resistance of a Ship". *The London, Edinburgh, and Dublin Philosophical Magazine and Journal of Science*, ***45***(272), pp. 106–123. Series 5.

[11] Peng, H., 2001. "NUMERICAL COMPUTATION OF MULTI-HULL SHIP RESISTANCE AND MOTION". PhD thesis, DALHOUSIE UNIVERSITY.

[12] Gourlay, T., and Dawson, E., 2015. "A Havelock Source Panel Method for Near-Surface Submarines". *Journal of Marine Science and Application*, ***14***(3), pp. 215–224.

[13] Doctors, L. J., and Beck, R. F., 1987. "Convergence prop-

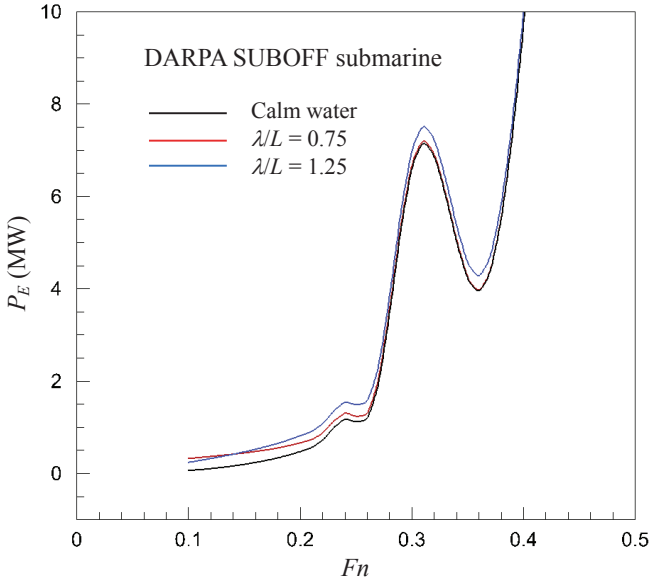

FIGURE 13: EFFECTIVE POWER P_E VS. FROUDE NUMBER IN REGULAR DEEP WATER WAVES FOR THE DARPA SUBOFF AT SUBMERGENCE DEPTH $d/D = 1.1$.

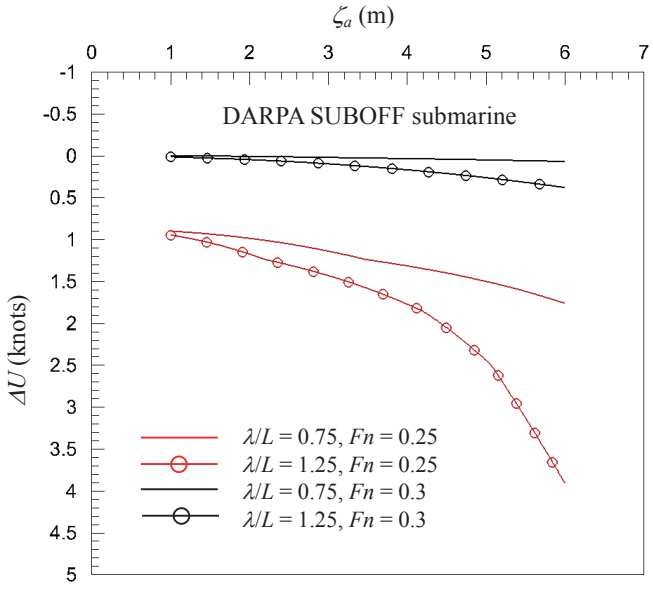

FIGURE 14: SPEED LOSS OF THE DARPA SUBOFF AT SUBMERGENCE DEPTH $d/D = 1.1$, FROUDE NUMBERS: $Fn = 0.25$ AND 0.3.

erties of the Neumann-Kelvin problem for a submerged body". *Journal of Ship Research,* ***31***(4), pp. 227–234.

[14] Havelock, T. H., 1932. "The Theory of Wave Resistance". *Proceedings of the Royal Society of London,* ***138***(835), pp. 339–348. Series A.

[15] Newman, J. N., 1987. "EVALUATION OF THE WAVE-RESISTANCE GREEN FUNCTION, PART 2: THE SINGLE INTEGRAL ON THE CENTERPLANE". *Journal of Ship Research,* ***31***(3), pp. 79–90.

[16] Söding, H., 2012. "Towards Fully Non-linear Floating Body Simulations by a Potential Method". In ASME 2012 31st International Conference on Ocean, Offshore and Arctic Engineering, American Society of Mechanical Engineers, pp. 539–549.

[17] Faltinsen, O. M., 2007. *Hydrodynamics of High-Speed Marine Vehicles*. Cambridge Univ. Press, Cambridge.

[18] Farell, C., 1973. "On the Wave Resistance of a Submerged Spheroid". *Journal of Ship Research,* ***17***(3), Mar., pp. 1–11.

[19] Farell, C., and Guven, O., 1973. "On the experimental determination of the resistance components of a submerged spheroid". *Journal of Ship Research,* ***17***(2), Feb., pp. 72–79.

[20] Lagally, M., 1922. "Berechnung der Kräfte und Momente, die strömende Flüssigkeiten auf ihre Begrenzung ausüben.". *ZAMM-Journal of Applied Mathematics and Mechanics/Zeitschrift für Angewandte Mathematik und Mechanik,* ***2***(6), pp. 409–422.

[21] Hundemer, J., 2013. "Entwicklung eines Verfahrens zur Berechnung der instationären potenzialtheoretischen Propellerumströmung". PhD thesis, Hamburg University of Technology.

[22] Katz, J., and Plotkin, A., 2001. *Low-Speed Aerodynamics*. Cambridge University Press.

[23] Ferreira Gonzales, D., Bechthold, J., and Abdel-Maksoud, A., 2017. "APPLICATION OF A BOUNDARY ELEMENT METHOD FOR WAVE-BODY INTERACTION PROBLEMS CONSIDERING THE NONLINIEAR WATER SURFACE". *ASME 2017 36st International Conference on Ocean, Offshore and Arctic Engineering*(OMAE2017-61852).

[24] Greve, M., 2015. "Non-viscous Calculation of Propeller Forces under Consideration of Free Surface Effects". PhD thesis, Hamburg University of Technology.

[25] Vaz, G., Toxopeus, S., and Holmes, S., 2010. "CALCULATION OF MANOEUVRING FORCES ON SUBMARINES USING TWO VISCOUS-FLOW SOLVERS". In ASME 2010 29th International Conference on Ocean, Offshore and Arctic Engineering, American Society of Mechanical Engineers, pp. 621–633.

[26] Toxopeus, S., Atsavapranee, P., Wolf, E., Daum, S., Pattenden, R., Widjaja, R., Zhang, J. T., and Gerber, A., 2012. "COLLABORATIVE CFD EXERCISE FOR A SUBMARINE IN A STEADY TURN". In ASME 2012 31st International Conference on Ocean, Offshore and Arctic Engineering, American Society of Mechanical Engineers, pp. 761–772.

[27] Ferziger, J. H., and Peric, M., 1999. *Computational Methods for Fluid Dynamics*.

[28] Hirt, C. W., and Nichols, B. D., 1981. "Volume of Fluid (VOF) Method for the Dynamics of Free Boundaries". *JOURNAL OF COMPUTATIONAL PHYSICS,* ***39***(1), pp. 201–225.

[29] Pinkster, J., 1980. "Low Frequency Second Order Wave Exciting Forces on Floating Structures". Phd thesis, Mechanical, Maritime and Materials Engineering, TU Delft, Oct.

[30] Standing, R. G., Dacunha, N. M. C., and Matten, R. B., 1981. Mean wave drift forces: Theory and experiment. Technical report R124, National Maritime Institute, Dec.

[31] Groves, N. C., Huang, T., and Chang, M. S., 1989. Geometric characteristics of DARPA suboff models (DTRC Model Nos. 5470 and 5471). Tech. Rep. DTRC/SHD-1298-01, David Taylor Research Centre.

[32] Havelock, T. H., 1931. "The Wave Resistance of a Spheroid". *Proceedings of the Royal Society of London. Series A, Containing Papers of a Mathematical and Physical Character,* ***131***(817), pp. 275–285.

[33] Wilson-Haffenden, S., Renilson, M., Ranmuthugala, D., and Dawson, E., 2010. "An Investigation into the Wave Making Resistance of a Submarine Travelling Below the Free Surface". In PACIFIC, Engineers Australia, pp. 370–379. International Maritime Conference 2010.

[34] Dawson, E., 2014. "An Investigation into the Effects of Submergence Depth, Speed and Hull Length-to-Diameter Ratio on the Near-surface Operation of Conventional Submarines". PhD thesis, University of Tasmania.

[35] Faltinsen, O. M., Minsass, K., Liapis, N., and Skjrdal, S. O., 1980. "Prediction of Resistance and Propulsion of a Ship in a Seaway". In Proceedings of the 13th Symposium on Naval Hydrodynamics, Office of Naval Research, p. 505529.